Determining hematite content from NUV/Vis/NIR spectra: Limits of detection

William Balsam[1,*], **Junfeng Ji**[2], **Devon Renock**[1], **Bobby C. Deaton**[3] and **Earle Williams**[4]

[1]Department of Earth Sciences, Dartmouth College, Hanover, NH 03755, USA

[2]Key Laboratory of Surficial Geochemistry, Ministry of Education, School of Earth Sciences and Engineering, Nanjing University, Nanjing 210093, China

[3]Department of Physics, Texas Wesleyan University, Fort Worth, TX 76105, USA

[4]Parsons Laboratory, Massachusetts Institute of Technology, Cambridge, MA 02139, USA

*Email: wbalsam@tds.net

Abstract

Hematite occurs in a variety of geologic settings including igneous, metamorphic and sedimentary rocks as well as in soils. However, it frequently occurs at low concentrations, especially in soils, where it may be less than 1% by weight. Because hematite has the potential to be an indicator of oxidizing and climatic conditions in soils and paleosols, it is important to understand its limit of detection. In this paper we examine the limits of detection of hematite visually and with diffuse reflectance spectrophotometry (DRS) and X-ray diffraction (XRD). To accomplish this we used a sample set consisting of "knowns" or calibration samples. These known samples consisted of 15 different matrices of varying mineral composition into which hematite in 7 different concentrations ranging from 0.01% to 4% by weight were mixed. Including the 0% hematite, our calibration dataset consisted of 120 samples. Visually, hematite can be detected at a concentration of 0.01% by weight in a light matrix and 0.5% in the darkest of our matrices. However, because of metamerism, visual techniques cannot specifically identify hematite. We find that for both DRS and XRD the limit of detection is also dependent on the matrix. For XRD the limit of detection for hematite in bulk samples is about 1%. For DRS the

limit of detection depends on the data reduction technique used. The commonly used Kubelka-Munk remission function and its first and second derivatives can easily identify hematite at the 0.5% level. However, the first derivative of the percent reflectance curve can detect hematite at 0.01% by weight in a light matrix and 0.05% in a dark matrix. We suggest that the first derivative of DRS curves is the best currently available method for qualitatively detecting the mineral hematite at low concentrations found in soils, sediments and rocks.

Work described in this paper may be applied in a number of situations. Our study of visual limits of hematite detection should aid field geologists in assessing hematite content. Analysis of color wavelength bands may also have application in remote sensing by indicating which bands are most sensitive to hematite, reported to be an important constituent of the Martian surface. Further, this study could help clarify remotely-sensed terrestrial albedo changes, especially the Sahara/Sahel transition where the sediments change from light, quartz-dominated to dark, hematite-dominated. Our study also points out that with laboratory-based spectra the first derivative of the reflectance curve is the most sensitive transform for processing spectral data for hematite, thereby allowing concentrations as low as 0.01% to be detected.

Keywords (as specified by journal): OPTICAL SPECTROSCOPY: hematite, XRD DATA: hematite, NEW TECHNIQUE: first derivative transform

Introduction

Iron oxides and oxyhydroxies are important geological materials. They are common weathering products and are widespread in soils and rocks. Not only are they economically significant, forming one of the bases of the industrial age, but they also preserve a variety of environmental information, making them potentially important proxy monitors of past

conditions. Iron oxides are important in remote sensing, especially of Mars, where they are thought to be responsible for the red color (Morris et al. 1997) and have been used to suggest the presence of water (Christensen et al. 2001). They occur as iron II (wusite), iron II, III (magnetite), iron oxide III (hematite) and iron III oxide-hydroxide (goethite). Although there are numerous iron oxide and oxide-hydroxide minerals, the most common on the Earth's surface are hematite (α-Fe_2O_3) and goethite (α-FeOOH) and their polymorphs maghemite (γ-Fe_2O_3) and lepidocrocite (γ-FeOOH).

Iron oxides can be powerful coloring agents (Deaton and Balsam 1991) and are commonly used as pigments in paints and other products. The color imparted by iron oxides can be far greater than their weight concentration implies making color a rapid and accurate indicator of oxidizing conditions (Schwertmann 1987). Iron oxides in ancient soils have also been suggested as indicators of paleorainfall and temperature (Kampf and Schwertmann 1983; Schwertmann 1987; Schwertmann and Taylor 1989; Torrent and Baron 2002; Balsam et al. 2004; Zhang et al. 2007). However, widespread use of iron oxides for paleoenvironmental analysis has yet to be fully realized. At least in part this is because iron oxides are usually present in low concentrations in soils, frequently 1% or less; making quantitative mineral analysis difficult (Balsam et al. 2004).

Typically, iron oxide mineralogy is determined by X-ray diffraction (XRD; Brown and Wood 1985). But, the lowest concentration of any particular iron oxide mineral (limit of detection) that can be identified by XRD without some enrichment procedure is about 1% by weight (Deaton and Balsam 1991) depending on the matrix composition and complexity (the matrix effect). Whereas other techniques, X-ray fluorescence (XRF) or atomic absorption spectrometry (AA) for example, can determine the concentration of elemental iron at very low

levels, few techniques can identify iron oxide mineralogy at low concentrations. Surprisingly some evidence (Deaton and Balsam, 1991) suggests that visually hematite can be detected at concentrations lower than with XRD, but this has not been rigorously investigated. However, the human eye is a qualitative instrument and color, the eye's perception of reflected light in the visible portion of the electromagnetic spectrum (400 – 700 nm), is the result of spectral mixing which may lead to the same color being produced by a variety of mineral mixtures, that is, metamerism. Hence, while color may provide hints about composition, it is not a unique determinant. Spectrophotometers, however, are at least as sensitive to iron oxides as the human eye and are not subject to the human eye's vagaries of spectral mixing (Deaton and Balsam, 1991). But, like XRD the nature of the matrix also affects a spectrophotometer's limit of detection. Although Deaton and Balsam (1991) examined the basics of iron oxide detection by reflectance spectrophotometry, their study used a limited number of samples (24), matrices (4) and range of iron oxide concentrations (0.01 – 1%). Further, they did not examine data enhancement techniques other than first derivatives.

At present, diffuse reflectance spectrophotometry (DRS) is a useful qualitative technique for identifying hematite, but the method would be more useful if quantitative information could be extracted from spectra. The ultimate goal of our research is to extract weight concentration of hematite from DRS spectra. As a first step, in this paper we examine the limits of detection of hematite in a variety of matrices using the human eye (visually), XRD and with a near ultra-violet (NUV), visible (Vis) and near infrared (NIR) spectrophotometer. In the process we examine the relationship between color bands and hematite content, the sensitivity of different data transforms to varying hematite concentrations and revisit the detection limit of hematite with a modern XRD and computerized data reduction software. To accomplish this, a set of

calibration samples or "knowns" was prepared. The calibration samples contained hematite in 7 concentrations ranging from 0.01% to 4% by weight. That is, from a concentration barely detectable with the human eye to a high soil concentration (Torrent et al. 1983). Fifteen matrices were spiked with the 7 different concentrations of hematite resulting in a total of 120 calibration samples including the matrix with 0% hematite (Table 1). In this paper, the focus is on hematite as opposed to both hematite and goethite because goethite can easily be determined by thermally oxidizing it to hematite and because hematite is a more powerful coloring agent than goethite (Zhou et al. 2010).

Previous Work

The scientific understanding of light and color goes back to Isaac Newton (1672) who demonstrated that white light could be separated into its component colors and that color is a function of light's wavelength. However, it was Goethe (1810) who suggested that color depended not only on the wavelength of light but also the physiology of human vision. The first system based on rigorous scientific experiments and able to express color with consistent alphanumeric descriptors was that of American artist and Professor Albert H. Munsell (1905). Munsell's color system was highly successful and was adopted by the USDA for soil research in the 1930's. It is still important today as a means of describing color in a wide variety of materials (Laamanen et al. 2005). The Munsell color system has been challenged and to some extent supplanted by the International Commission on Illumination's CIELAB (L*a*b*) and CIECAM02 color models. (For a thorough description of CIE color space consult http://www.cie.co.at/main/freepubs.html.) Both the Munsell and CIE systems allow color to be measured numerically with a colorimeter which gives more consistent results than the human eye (Torrent et al. 1983; Deaton 1987). However, both the Munsell and CIE measures are designed

to mimic human vision. As a result both are subject to the same limitations as human vision, metamerism. This limitation is overcome by using a reflectance spectrophotometer, a machine that records percent reflectance relative to a pure white standard. It is possible to quantify color from a sample's visible light spectrum, but, because of metamerism, the Vis spectrum may not be determined from a sample's color. Hence, in reducing a spectrum to color, information is lost (Barrón and Torrent 1986). In this paper we focus on the use of a NUV/Vis/NIR spectrophotometer to identify the mineral hematite. However, we also recognize that the eye can discern hematite at very low levels and develop some guidelines for geologists to use in the field to estimate hematite content.

Winters (1930, as referenced in Shields et al. 1968) was perhaps the first to use a colorimeter/spectrophotometer to analyze geological material, in this case soil. Prior to 1986 spectrophotometers were used mainly as colorimeters to produce data to quantify either Munsell or CIE colors (see for example Torrent et al. 1983). With the advent of computer-controlled spectrophotometers, the recording of data became easier and more accurate. Barrón and Torrent (1986) were the first to use a spectrophotometer with digital data recording to analyze geological materials.

A number of techniques have been proposed to extract component concentration (weight percent) from spectral data; none succeeds under all circumstances and most fail in complex geological environments, e.g. soils. These techniques include color bands, the Kubelka-Munk remission function and the first and second derivative of this function, log transforms and first derivatives of the percent reflectance curve. Perhaps the first non-color based technique used to unmix spectra and one still widely used today is the Kubelka-Munk (K-M) remission function (Kubelka and Munk 1931; Kubelka 1948). The equation for the remission function is (Eq. 1):

$$f(R) = \frac{(1-R)^2}{2R} = \frac{k}{s} \quad \text{(Eq. 1)}$$

where:

R= 0.01 times the percent reflectance at a specific wavelength

k = molar absorption coefficient

s= the scattering coefficient

Log transforms of spectral data are popular in some industries (Hsu 1997). The most common log transform is the log (1/R), where R is reflectance. However, according to (Clark and Roush 1984; Clark 1999) this is less robust than the older Kubelka-Munk function. Log transforms will not be considered further in this study.

To our knowledge the first publication to suggest the use of the first derivative of the percent reflectance curve to identify hematite was Barranco et al. (1989) who also demonstrated that the wavelength position of the first derivative peak for hematite is a function of concentration and the peak wavelength gets longer as the concentration increases. Balsam and Deaton (1991) confirmed this observation and noted that, although hematite exhibits several absorption bands in the Vis and NIR, only the Vis absorption band [the result of an electron pair transition (Scheinost et al. 1998)] persists when the hematite concentration falls below 2% (Balsam and Deaton 1991). The first derivative peak for the Vis absorption band appears unique to hematite. We know of no common minerals that show a peak at this wavelength.

Deaton and Balsam (1991) published the first truly systematic investigation of the limits of detection of different concentrations of hematite and goethite in a variety of matrices by diffuse reflectance spectrophotometry. They used the first derivative to identify hematite and goethite both of which they investigated in concentrations from 0.01% to 1% by weight and in four

different matrices. [Table 1 in Deaton and Balsam (1991) contains details of the simulated matrices]. From these systematic experiments two characteristics of Vis spectra with hematite and goethite were evident. First, if matrix composition was held constant the height of the first derivative peak was a good indicator of either hematite or goethite concentration. [Note, Balsam and Deaton (1991) indicated that at some concentration above 1% the first derivative peak height for hematite decreases and is accompanied by an increase in the wavelength of the peak.] Second, as matrices become darker and possibly more complex, the height of first derivative peaks for identical concentrations of hematite is reduced. Taking these two observations into account Deaton and Balsam demonstrated that even under the most difficult circumstances it is possible to detect hematite at a weight concentration of 0.03% and goethite at 0.05% by weight. The matrix effect in hematite spectra was first noted by Morris and Lauer (1990), although they used matrices not typical of mixtures found on Earth.

Scheinost et al. (1998) applied the second derivative of the K-M function to soil samples, and noted that the minimum concentration of hematite they could easily detect was about 0.5%. They did not systematically test different concentrations of hematite in a variety of geological matrices. Nevertheless, they did provide a theoretical basis for the use of derivatives to identify different iron oxides, especially hematite and goethite, from reflectance spectra.

Materials and Methods

Materials

To assess if weight percent hematite can be determined from NUV/Vis/NIR spectra, a data set of 120 samples (Table 1) with known concentrations of hematite in varying matrices was created with a combination of manufactured and natural materials (Table 2). Manufactured materials were used for hematite, calcium carbonate and silica; natural materials were used for

illite, chlorite, kaolinite and montmorillonite. Manufactured materials have the advantage of having a known composition and consistent physical characteristics with no contaminants. All the manufactured materials were micron or sub-micron in size. For hematite the color is indicative of the grain size. Only hematite crystals <~0.1 microns are red in color (Cornell and Schwertmann 2003); coarser crystals ~0.4 microns are purple and those >~0.5microns are gray or black. The dominant color of hematite in terrestrial soils and rocks is red suggesting most natural hematite is also sub-micron size. Because reflectance spectrophotometry does not depend on reflections from crystal planes, small crystal size is not a problem for DRS as it can be for XRD. All our clay mineral samples, which are natural materials, might better represent what is found in soils and sediments. But, they typically have a range of compositions and are rarely pure. That is, natural materials, even our clay mineral standards, include a variety of other minerals. All our clay mineral standards were pulverized in a ShatterBox® swing mill to a grain size of about 10 microns (http://www.spexsampleprep.com/products_by_category.aspx?cat=5).

Hematite concentrations included 0.0, 0.01, 0.05, 0.1, 0.5, 1, 2 and 4 percent by weight. These hematite concentrations encompass the range found under natural conditions in many soils and paleosols (Balsam et al, 2004). We used 5 base matrices into which different minerals were added for a total of 15 different matrices (Table 1). These matrices ranged from light ones based on calcium carbonate or silica and darker matrices that included illite and chlorite. The base matrices included calcium carbonate, silica, carbonate and silica mixed 1:1, a matrix designed to resemble North Atlantic deep-sea sediment and a matrix that simulates Gulf of Mexico sediment. Carbonate and silica are typical of sediments found on the Earth's surface with carbonate being the basis of soil developed on limestone terrains and silica being typical of terrain formed on both igneous rocks and clastic sedimentary rocks. Silica is also typical of some desert sediments,

especially the Sahara, and the investigation of silica with varying concentrations of hematite might be useful in modeling albedo changes from the Sahara (white, quartz-rich) to the Sahel (red, hematite-rich). The simulated North Atlantic matrix contains silica, carbonate, and illite in the ratio 4/3/3. To this simulated North Atlantic matrix we add 1, 5 and 15% chlorite. The Gulf matrix contains carbonate, silica, and illite in the ratio 5/3/2. To the Gulf matrix we added 1, 5 and 15% kaolinite and 1, 5 and 15% montmorillonite. We chose to model North Atlantic and Gulf of Mexico sediments because the North Atlantic receives sediments that have undergone substantial physical weathering whereas the Gulf of Mexico receives sediments that have been subjected to significant chemical weathering. Our mineral ratios are based on work by Biscaye (1965) and Griffen (1962) which provided the clay mineralogy of North Atlantic and Gulf of Mexico sediments, respectively.

It is important to note that none of our calibration samples include organic matter. As noted by Balsam and Damuth (2000), characterizing organic material spectrally is difficult because the composition and color of organic material is highly variable. The precise pattern produced by organic matter is a function of the type of organic material, especially how refractory the organic matter is, and its concentration. Hence few generalizations about organic material are possible. However, Balsam and Wolhart (1993) and Deaton and Balsam (1996) noted that as organic material gets darker it seems to conceal the signal of iron oxides by causing absorption through much of the Vis.

Methods

Visual Detection. The visual detection limit of hematite in our various matrices was tested by assembling a set of 20 samples ranging in hematite content from 0 to 0.5% and with matrices that were both light and dark. (All samples with more than 0.5% hematite were sufficiently red

that there was no reason to test them.) The samples were placed in clear plastic vials randomly numbered from 1 to 20. Volunteers including geology students, artists and average citizens were asked to rate the degree of redness from none to slight to moderate to intense. Samples were drawn one at a time from an opaque cloth bag, the degree of redness was determined through the plastic vial in sunlight at various times of day, and the sample placed in a different opaque cloth bag before another sample was analyzed. This procedure was followed until the degree of redness of all 20 samples was determined.

Sample Preparation. The powdered samples were mixed by grinding in a synthetic sapphire mortar and pestle. To ensure that components were sufficiently dispersed, a subset of samples was subjected to a milling step in a McCrone micronizing mill for 10 minutes with methanol. Reflectance spectra from ground and micronized samples were similar suggesting that grinding adequately dispersed all sample components. The chief difference between the samples was that the micronized samples tended to be slightly (~3%) lighter from 350 – 550 nm. For wavelengths longer than 550 nm the curves were within <1% of each other.

After grinding the samples were placed on glass slides, made into a slurry with distilled water and allowed to dry at room temperature. The sediment on the resulting slides was thick enough that light could not pass through, that is, the slides were opaque, and looked like thick XRD slides (Figure 1 a and b). As noted by Balsam and Deaton (1991) grinding samples not only enhances the ability to make slides, but also diminishes any grain size and surface roughness effects.

X-ray Diffraction. To provide a standard technique for the measurement of hematite concentration for comparison with spectrophotometry, XRD was used on five powder samples. These samples contained 0, 0.01%, 0.1%, 1.0%, and 4.0% Fe_2O_3 by weight in the Gulf matrix

with 1% kaolinite. Each sample was mixed with 10% ZnO and a slurry of solid + iso-propyl alcohol was produced. ZnO was added as a reference standard to assess shifts in diffraction peak position. Each slurry was then ground in a McCrone micronizing mill at the University of Vermont for 10 minutes. Wet milling in methanol using a McCrone micronizing mill is a widely applied technique for quantitative XRD analysis (Moore and Reynolds 1997). The method has been proven to produce a narrow, nominally <10 μm, particle size distribution (O'Connor and Chang 1986; Hillier 2003; Dermatas et al. 2007) while only introducing a minimum of structural damage. Since these powders were prepared from manufactured and natural materials, the milling step was primarily used to ensure heterogeneity within the powders. Samples were dried and loaded in a powder XRD sample holder via a backpacking method to minimize preferred orientations in the packed-powder bed.

X-ray spectra were obtained using a Bruker D8-Focus diffractometer at Dartmouth College. The powdered samples were run from 2 to 70 degrees two theta at 40 KV and 40 Ma (0.01 degree step increments at 2 seconds/step). The X-ray data were analyzed using Bruker EVA pattern processing software.

Reflectance Spectrophotometry. Sample slides were analyzed in a Perkin-Elmer Lambda 6 NUV/Vis/NIR spectrophotometer with a diffuse reflectance sphere. This instrument records percent reflectance as a function of wavelength from 250 – 850 nm relative to a white, barium sulfate standard. Samples were analyzed using a slit width of 2 nm and scanned at a rate of 600 nm/min. Total analysis time per sample was 2 to 3 min. Data were collected at 1nm intervals and written directly to a computer file. As reported by Balsam et al. (2011), data from the Lambda 6 are reproducible to +/-1%.

Diffuse reflectance spectrophotometry has many advantages compared to visual methods of mineral identification, that is, color. Spectrophotometers are not affected by metamerism and, unlike the vagaries of human perception of reflected light, they are consistent and precise. Further, with laboratory-based spectrophotometers the wavelength of the light source can be precisely controlled and, with the reflectance spheres used in DRS, the angle of the light reflected from a sample is not an issue. However, spectrophotometers are limited in a number of ways. All spectrophotometers produce results that are reflectance value as a function of wavelength. Individual values are highly dependent on surrounding values resulting in data with strong serial correlations that must be taken into account in statistical hypothesis tests. Further, as the spectrophotometer scans a sample's surface, what it measures is more a function of percent of surface area than weight. In practical terms, this means that materials with a high density might be more difficult to identify than materials with a low density. Where density plays a major role is with organic material that in soils commonly has a very low density [<0.9 – 1.3, (Pilatti et al. 2006)] compared to mineral components (frequently 2.6 – 2.75). This means that a small weight percent organic material can have a major impact on the character of a spectrum by dominating the surface area (Balsam and Wolhart 1993).

Spectral Data Reduction. DRS data were processed in several ways. The first parameter calculated was optical lightness, also called luminance (L*), grayscale, albedo, or average reflectance (see Balsam et al. 1999 for details). Percent reflectance in each of the color bands following the color divisions of Judd and Wyszecki (1975) was also calculated. For example, for the red color band, the percent reflectance values were summed from 630 to 700 nm, divided by the optical lightness and multiplied by 100.

We also calculated changes in the slope of the percent reflectance curve by taking the first derivatives of the reflectance data as percent per nanometer and recorded the wavelength as the mid-point of the 10nm calculation interval. First derivatives, as shown below, are more amenable to interpretation than the untransformed reflectance spectra; the first derivative curves contain more peaks compared with reflectance curves which tend to be smoother and change more gradually. Barranco et al. (1989), Deaton and Balsam (1991), Balsam and Deaton (1991), and Balsam and Damuth (2000) have demonstrated that the position of peaks and valleys on the first derivative curves are indicative of sediment composition and mineralogy. Finally we determined the K-M function for the reflectance spectra and calculated the first and second derivative of that function. Scheinost et al, (1998) indicate that the derivatives of the K-M function are useful for quantifying hematite and goethite content.

Results

Visual Results

One purpose of this study is to document the sensitivity of the human eye with respect to hematite in varying matrices. Although Clark (1999) indicates the eye acts as a crude spectrophotometer, there has been little work that systematically demonstrates its sensitivity to different minerals under controlled conditions. Further, as noted above, the analogy to a spectrophotometer is imperfect because the eye records only red, green and blue and not reflectance at specific wavelengths as a spectrophotometer does. Despite metamerism, we note that for soils and sediments, hematite is by far the most common mineral capable of producing a red color or cast (A. Alden http://geology.about.com/od/mineral_ident/tp/Red-Pink-Minerals.htm). Hence, a red color in geological material and particularly in soils likely correlates with the presence of hematite.

Results of the visual discrimination of hematite are shown on Table 3. This table illustrates both the strengths and weaknesses of human vision. In calcium carbonate or carbonate/silica – hematite was easily distinguished by eye at very low levels, ~ 0.01% by weight. For calcium carbonate 95.8% of the participants identified 0.01% hematite whereas for carbonate/silica 62.5% of the participants identified 0.01% hematite. Other results exhibit the vagaries of human vision with inexplicably only 95.8% of participants identifying redness in 0.1% hematite and carbonate and some participants seeing red where no hematite was present in carbonate/silica, North Atlantic and Gulf matrices. For the Gulf matrix, hematite is consistently observable at a concentration of 0.1%; for the North Atlantic matrix the hematite is not consistently observable until it reaches a concentration of 0.5%.

Clearly hematite is more easily distinguished in light matrices (carbonate or carbonate/silica) than in the darker matrices. Of these light matrices, hematite is clearly more evident in calcium carbonate than in carbonate/silica or silica. Despite both calcite and silica being very white, and their average albedo similar - about 90% for carbonate and 87% for silica - hematite is clearly more evident in carbonate. Further, at higher percentages hematite has an orange cast in the silica matrix compared to the typical brick red seen in calcite. A matrix consisting of a 1:1 mixture of carbonate and silica produces results in between the two pure matrices and the color at higher percentages has a slight orange cast (Figure 1a). These observations suggest that in terms of color, the mixing of minerals is a complex process likely involving differences in refractive indices as well as ability to transmit light (Morris and Lauer 1990).

As illite is added to this 1:1 carbonate/silica matrix the limit of detection of hematite increases; for 50% illite the detection limit is ~0.1% (Table 3, Figure 1a). This change in

detection limit is paralleled by a change in sample darkness; 1:1 carbonate/silica with no hematite has an albedo of 87%; for 50% illite the albedo decreases to 35%. For a matrix containing 15% chlorite the detection limit falls even further to 0.5% (Table 3, Figure 1b). However, hematite itself also significantly darkens a sample; as hematite concentration increases samples get darker. Hence, dark samples of similar reflectivity may be produced by either a dark matrix, increased hematite or both. It must be emphasized that many of the color changes noted above are subtle and, were it not for the series of samples presented here, might not be as easily distinguished.

XRD Results

The X-ray diffractometer technique is well-documented for iron oxides (Bigham et al. 1978), but the limits of detection in different matrices (e.g., soils and sediments) are not rigorously defined. Interpretation of diffractograms from mixtures with many minerals is not straightforward since they contain the diffraction peaks for the mineral matrix and hematite. We show a representative portion of a diffraction pattern (Figure 2) for a synthesized deep-sea sediment matrix that is moderately complex and of average albedo, Gulf with 1% kaolinite (Table 1) containing 1% hematite. At a concentration of 4% by weight, hematite is unequivocally identifiable (not shown). However, the hematite peaks are barely visible at a concentration of 1% (Figure 2) and are not present at 0.1% concentration (not shown). At 1% concentration, although the peaks indicative of hematite are present, without an *a priori* knowledge they probably would not be interpreted as indicative of hematite.

Diffuse Reflectance Spectrophotometry Results

As indicated above, many transforms have been used to extract compositional information from spectra. We first examine the nature of percent reflectance spectral curves (raw data) of samples

containing hematite and then assess if a single transform can accurately represent hematite concentration in varying matrices. We limit this investigation to commonly used single variables or ratios of single variables. Variables to be investigated include color bands and their ratios, first derivatives, Kubelka-Munk remission function, and the first and second derivative of the K-M function.

Raw NUV/Vis/NIR Spectral Data. A number of features are obvious from the raw reflectance curves. We use examples of a light matrix, calcite plus silica, and a dark matrix, North Atlantic plus 15% chlorite (Figures 1a and b), but results from matrices of comparable lightness are similar. For both the light matrix and the dark matrix it is clear that hematite produces a characteristic reflectance change between 550 and 600 nm. In the light matrix this change is evident even with as little as 0.01% hematite (Figure 3 a). Clearly the spectrophotometer is capable of detecting hematite at concentrations as low as the human eye. For the darker matrix, 0.01% hematite simply darkens the sample without the distinctive decrease from 550 -600 nm. The hematite signal in this darker matrix becomes evident at values >0.01% and is fully apparent at 0.5% by weight, about the same hematite concentration the eye can distinguish in this matrix (Figure 3 b).

In addition to the change in reflectance between 550 and 600 nm, for each matrix there is a predictable pattern of change. In each matrix set, as hematite concentration increases the samples get darker (lower overall reflectance) and the decrease from 550 -600 nm becomes more pronounced (Figure 3). This pattern is repeated in every matrix set evaluated. There is also a tendency for the change in reflectance from 550 -600nm to be offset to longer wavelengths as the hematite concentration increases.

All these variations corroborate the view of Deaton and Balsam (1991) and Ji et al. (2002) that if matrix is held constant it is possible to estimate hematite content from the Vis spectrum. However, these curves also indicate that changes in matrix composition might make it difficult to estimate hematite concentration when the matrix composition varies.

Color Bands. Perhaps the most straightforward method of reducing spectral data is through the use of color bands. Color bands and the ratio of color bands are widely used to interpret data from space-borne spectrophotometers with experience determining how each band can be used for identifying specific conditions (http://landsat.usgs.gov/best_spectral_bands_to_use.php). Given the color of hematite, percent reflectance in the red color band could be a potentially useful variable. However, color bands are difficult to test for limits of detection because any substance that changes the spectral curve will alter the percent in a color band. Instead of actually testing the limit of detection, we examine the relationship between color band and percent hematite. To assess red color band reflectance as an indicator of hematite, we plotted %hematite vs. %reflectance in the red color band (Figure 4) for the 7 matrix sets shown in Figure 1a and b. The resulting plots indicate that the relationship between % hematite and %red within each matrix set is an exponential growth curve (Figure 4a). But, for different matrix sets the curves differ significantly. The curves also show that as hematite concentration increases %red values for the different matrix sets show significant variation. As a result a %red value of ~38% could be indicative of hematite values from 1 – 4% (Figure 4b). For each individual matrix set (Figure 4a), however, the curves are remarkably consistent with all the illustrated curves having an r^2 >0.99 and a standard error of estimate (SEE) <0.095. Clearly, if the matrix is held constant it would be possible to accurately estimate hematite content from the percent in the red color band. However, when all 120 test samples are grouped into a single data set, the r^2 falls to 0.822

and the SEE increases to +/-0.559 (Figure 4b). Although the r^2 is relatively high, an SEE of +/-0.559 indicates that it would be difficult to detect hematite confidently at concentrations <~0.5%, making the equation unusable for many soils and sediments. Of all the color bands, percent in the orange color band (Figure 4c), has the highest r^2 and lowest SEE when regressed against hematite concentration.

First Derivative Values. Our data confirm that hematite produces a very distinctive first derivative signature. This signature is a peak in the first derivative curve between 555 and 585 nm. In both of the mixture series (Figure 5) this peak is evident and confirms that in light matrices (calcite and silica, Figure 5a) the limit of detection of hematite with first derivative values is <0.01% by weight. However, in darker matrices, the North Atlantic with 15% chlorite for example (Figure 5b), the detection limit of hematite is 0.05%, a concentration that is lower than can be resolved by the human eye.

The mixture series (Figure 5) clearly shows the matrix effect on reflectance spectra. Part of the matrix effect is to reduce the limit of detection in darker matrices as described above. In addition, the matrix effect also suppresses the height of the hematite first derivative peak. In a light matrix (Figure 5a) the first derivative peak has a maximum value of about 0.9 whereas in darker matrices that value is reduced to about 0.6 (Figure 5b). A darker matrix also completely suppresses a peak at about 700 nm and an absorption feature centered at <800 nm (Figure 5). As shown by Balsam and Deaton (1991) this absorption band, which is frequently used to identify hematite, completely disappears when hematite concentration falls below 2%. This paper further refines the above observation and demonstrates that for dark matrices the absorption band described in Figure 2 of Balsam and Deaton (1991) is not present. In addition, as hematite concentration increases the wavelength of the first derivative peak also increases. In a light

matrix the wavelength increases from 565 nm for 0.01% to 585 nm for 4.0% hematite whereas in a dark matrix it increases from 555 nm for 0.05% to 575 nm for 4% hematite.

Kubelka-Munk Remission Function. Following color bands, the Kubelka-Munk remission function is probably the most commonly used transform of spectral data. Although it has been applied to geological data, its sensitivity to diverse minerals has never been rigorously tested in data sets of different matrices with varying amounts of hematite. Figure 6 shows how the K-M function transforms the raw spectral data (%reflectance as a function of wavelength, Figure 3). As with the percent reflectance data (Figure 3), it is clear that hematite affects the K-M spectrum, especially from 500 – 600 nm. The K-M function compresses the curves at the red end of the spectrum and expands, reverses (light samples with 0% hematite have lower values and as hematite is added and samples get darker the values increase) and spreads out values at the violet end of the spectrum. K-M values in the light matrix (Figure 6a) indicate a potential problem; the 4 curves with hematite values ranging from 0 – 0.1% are virtually identical. However, for the dark matrix the values are more spread out at the violet end of the spectrum (Figure 6b).

Geological researchers generally do not use untransformed K-M values; rather either first or second derivative values are used. Figure 7 shows the first derivative values for the light and dark matrices. The first derivative of the K-M function exhibits patterns similar to the first derivative of the %reflectance curves with one important exception, the limit of detection for both the matrices increases to between 0.1% and 0.5%. (In both matrices the peak at 0.1% is so small that it is likely to be overlooked and 0.5% appears a more realistic detection limit.) For both matrices the limit of detection using the K-M function is at least 10 times greater than the amount that can be identified with the first derivative (Figure 5). Scheinost et al. (1998)

suggested that 0.5% is the lowest concentration of hematite that can be easily identified using the K-M function. Our work strengthens this conclusion. However, we cannot rule out the possibility that in some matrices the detection limit is lower, possibly only slightly >0.1% by weight.

Several researchers (Scheinost et al. 1998; and Torrent et al. 2007) have suggested that the second derivative of the K-M function provides useful data to characterize iron oxides from DRS spectra. Our data show that in both light and dark matrices the second derivative of the K-M function (Figure 8) has the same limit of detection as the K-M first derivative, that is, about 0.5%. Scheinost et al. (1998) also suggested that the ratio of the amplitude difference between the ~415 nm minimum and the ~445 nm maximum for goethite and the ~535 nm minimum and ~580 nm maximum for hematite is a good measure of the goethite to hematite ratio. The detection limit also applies to the amplitude of the difference from 535 – 580 nm which approaches 0 for hematite values less than 0.5%. Although this paper does not address the mineral goethite, Deaton and Balsam (1991) indicate that in dark matrices the detection limit for goethite is about 0.5%. Clearly, when using ratios of the K-M second derivatives to determine hematite to goethite ratios one must be careful to insure that the values are above the detection limit.

Discussion

For the field geologist and soil scientist this paper provides a method to assess fine-grained (sub-micron) hematite content visually. The detection limit of hematite by eye varies with the color, lightness and mineralogy of the matrix (Figures 1, 5). In light matrices such as quartz or calcite, hematite can be detected visually at concentrations as low as 0.01%. The addition of light minerals such as kaolinite and montmorillonite in a light matrix has little additional effect on the hematite detection limit. However, as the matrix darkens because of the addition of dark minerals

such as illite or chlorite, the detection limit increases reaching 0.1% to 0.5% by weight. The transition from light to dark matrices is also marked by a change in the character of the red color from intense and vibrant to muddy (Figure 9). Given some *a priori* knowledge of rock or sediment mineralogy field geologists and soil scientists should be able to use color to make a reasonable estimate of hematite concentration.

In addition to altering the detection limit, different minerals also change the color of the sample for the same concentration of hematite. With carbonate and silica matrices, despite the fact that both are very light, the hematite visually is more obvious in the carbonate matrix than in the silica matrix and the color of the samples in each of these white matrices differs with the silica samples being somewhat lighter and less saturated for a corresponding hematite concentration. Further, mixtures with chlorite and especially with high concentrations of illite tend to give the samples a decidedly brown cast. Hence, a reddish brown color and its Munsell/CIE equivalent is not just the result of different iron oxide minerals as indicated by Torrent et al (1983), but also the matrix in which they are found.

This change in color with matrix is well illustrated by our samples that contain 0.1% hematite (Figure 9). These samples range from red-orange to pink to various shades of brownish-red. Clearly, in samples with different matrices there is no consistent relationship between color and hematite content suggesting that Munsell or CIE color is not useful for identifying hematite concentration. Some efforts have been made to quantify color using the Munsell and CIE color systems. The seminal work with respect to hematite is that of Torrent et al. (1983) who first used data from spectrophotometers to calculate numerical color parameters based on tristimulus values which indicate the relative spectral sensitivities of the three types (R, G, B) of cone cells. They demonstrated a high degree of correlation (r^2) between numerical color parameters and

hematite content in specific soil types. However, they also demonstrated that when the soil type changed (that is matrix composition changed) a different regression equation was required or the correlation was significantly reduced. Hence, based on their data, it appears that a single equation is capable of estimating hematite content only if sample matrices are mineralogically similar. This view is also supported by our plot of percent red vs. hematite content (Figure 4), indicated by the plots of Deaton and Balsam (1991) and the data in this paper. Ji et al (2002) have since used the observation that if matrix is held constant, then the effect of changing hematite concentration is consistent and predictable. They showed that by chemically removing iron oxides from a natural matrix and then spiking that matrix with known concentrations of hematite and goethite it was possible to write equations based on DRS spectra that could accurately estimate hematite and goethite content in similar matrices.

Although there are significant differences in the data gathered by satellite-borne spectrophotometers and our laboratory instrument, bi-directional reflectance vs. diffuse reflectance and a significant thickness of atmosphere for satellites, the comprehensive nature of the dataset used in this study has the potential to be useful to those engaged in remote sensing. In remote sensing the amount of reflectance in a color band or the ratio of color bands is commonly used to determine composition. In this study we show that if matrix is held constant, percent in the red color band forms a predictable exponential growth curve from which hematite could be estimated (Figure 4a) with reasonable precision. However, when all the matrices are combined the r^2 of the red color band vs. hematite decreases and more importantly the SEE falls to +/-0.559 (Figure 4b) indicating the ability to detect hematite at concentrations less than about 0.5% is limited. We note (Figure 4c) that of all the color bands, orange is best at estimating hematite content and has a higher r^2 and lower SEE than the red band. In spectral analysis of remote

528 sensing data from satellite-borne spectrophotometers the ratio of (color) bands is frequently used;
529 the Landsat TM band 3/1 ratio (about red/blue) is reported to be indicative of iron oxides
530 (Sabins, 1999; Ji et al 2004). Our data, however, indicate that the green/red ratio is better at
531 discriminating hematite content. A plot of the green/red color band ratio versus %hematite
532 (Figure 10) again suggests a nonlinear relationship between these two variables and a regression
533 employing an exponential decay curve produces a higher r^2 and lower SEE compared to the red
534 color band (Figure 4b), but a lower r^2 and higher SEE compared to orange (Figure 4c).
535 Other transforms of the raw spectral data (Figure 3), that is, first derivative curves (Figure
536 5) or the Kubelka-Munk remission function and derivatives of it (Figure 6, 7, 8) were examined.
537 Of these two commonly used transforms, the first derivative of the percent reflectance curve is
538 clearly superior at detecting hematite. In light matrices, first derivatives can detect hematite at a
539 concentration of 0.01% by weight; in darker matrices hematite can be detected at a concentration
540 of 0.05% by weight with first derivatives. For the Kubelka-Munk remission function the lowest
541 detection limit documented in this study is ~0.5%, the same as in previous studies (Scheinost et
542 al, 1998). This high detection limit is consistent with the work of Simmons (1972) who warned
543 that marked deviations from theory have been observed when the K-M function is applied to
544 strongly absorbing materials, for example, hematite.
545 DRS first derivative curves' peak height is sensitive to hematite concentration (Figure 5).
546 But, peak height is also a function of matrix composition and therefore is not a reliable indicator
547 of hematite concentration in varying matrices. Further, it is clear that sample lightness must be
548 taken into account as it influences both the limit of detection and the height of the hematite first
549 derivative peak. These considerations suggest that the range in hematite concentrations in soils
550 and rocks cannot be adequately characterized with a single variable. In addition, our first

551 derivative curves suggest that trying to characterize the spectral response of hematite with a
552 single sample is inadequate because the spectral curve changes with both hematite concentration
553 and matrix mineralogy. This observation is especially true when trying to characterize hematite
554 from a pure sample. Comparison of our data to the spectral pattern of pure hematite (Barranco et
555 al. 1989) indicates that spectral patterns based on pure minerals are not likely to be reliable
556 indicator of absorption features in natural mixtures. A similar conclusion was reached by Morris
557 and Lauder (1990).

558 **Implications of this Research**

559 Iron is one of the more common elements on the Earth's surface. It is ubiquitous in its many
560 chemical forms in soils, sediments and rocks. On the surface iron is not only present in igneous,
561 metamorphic and clay minerals, but also, in the presence of oxygen, forms iron oxides and
562 oxyhydroxides that accumulate in soils and sediments. These oxide/oxyhydroxide minerals,
563 although visually quite evident from their color, occur in low concentrations and are difficult to
564 identify by conventional instrumental methods such as XRD. In this paper we demonstrate that
565 visual methods can effectively be applied to provide qualitative estimates (none, sparse,
566 common, and abundant) of hematite content. Further, we show that DRS has the capability of
567 providing semi-quantitative estimates of hematite content if matrix is held constant. This
568 information should be useful to mineralogists and in soil science, sedimentology, marine
569 geology, and paleoclimatology, fields in which DRS has already been applied with some success.
570 For the mineralogist this paper expands and reinforces previous studies. When the study of
571 Deaton and Balsam (1991) that compared XRD and DRS was published, the default technique
572 for detecting the presence and percentages of hematite in various matrices was XRD. The results
573 of this study with more up to date equipment and computer processing software confirms the

574 work of Deaton and Balsam (1991) that about 1% is the detection limit of hematite in a complex
575 matrix with XRD. The results of the original study indicated that DRS could improve on XRD in
576 terms of detection limits. The current, more thorough investigation indicates that the detection
577 limit with DRS is at least 100 times lower than XRD for a light matrix (Figure 5a), and at least
578 20 times lower in a dark/complex matrix (Figure 5b). Understanding this limit in typical
579 geological and soil environments is important because hematite is frequently less than 1%. We
580 also demonstrate that for DRS the data reduction technique is an important control on the limit of
581 detection. Using the popular Kubelka-Munk remission function the detection limit of hematite is
582 about 0.5%. But, by using the first derivative of the reflectance curve the detection limit lowers
583 to 0.01 – 0.05% depending on matrix. This study also indicates the importance of knowing the
584 limits of detection for both XRD and DRS when assessing output from computer programs to
585 avoid interpreting noise as data.

586 For the soil scientist or sedimentologist we document that the limits of detection of
587 hematite visually depends on the darkness of the matrix, that is, 0.01% in a light matrix and 0.10
588 to 0.50% in darker matrices. In addition, we provide some guidance for visual determination of
589 concentrations above the detection limit. We also note that qualitative visual estimates of
590 hematite content can be further refined through the use of a spectrophotometer to positively
591 identify hematite (the eye cannot distinguish between different red materials) and to provide
592 semi-quantitative estimates of hematite content with the use of first derivative curves. These
593 estimates are below the limit of detection of XRD. Qualitative estimates of hematite content have
594 also been used in marine geology to trace the dispersal of Saharan dust in the equatorial Atlantic
595 (Balsam et al, 1995) and the redistribution of terrestrial sediments by deep ocean currents
596 (Barranco et al., 1989). The data provided in this paper will help to further refine these estimates

and, through the use of appropriate first derivative curves based on sample albedo (dark, light, etc.), make semi-quantitative estimates possible. Enhanced identification of hematite could also be useful in paleoclimatic work. As noted earlier, the ratio of hematite to goethite has been used as an indicator of precipitation with hematite dominating in warm dry conditions and goethite in cooler, wetter conditions. Perhaps the easiest way to determine goethite concentration is by thermally oxidizing it to hematite and using the after and before difference to calculate goethite (Zhou et al. 2010). Because this work is the first step towards improving estimates of hematite concentration directly from spectra, it will also enhance determining goethite and hematite to goethite ratios that are potentially useful in paleoclimatic studies.

This work may also have application in remote sensing, especially of Mars where sub-micron hematite is thought responsible for the red color of some of the planet (Christensen et al. 2001). In this study the orange color band proved to be a useful proxy for moderate concentrations of red hematite, better than the ratio of color bands. Further, when attempting to characterize the spectrum of a mineral it is important to remember that the spectrum of a pure sample will likely differ from the spectrum of that mineral mixed with other components. Morris and Lauder (1990) reached a similar conclusion, but we emphasis that not only is difference in matrix composition important, but also that the albedo of the matrix has a major influence on the detection limit. Finally, if data quality from remote sensing instruments permits, first derivative curves have the potential to identify and quantify hematite at very low concentrations, depending on matrix composition.

Acknowledgments

This study was in part funded by the National Natural Science foundation of China through grants 41230526 and 41273111 to Ji. We thank Eric Posmentier and Justin Richardson for

620 comments and criticisms during the preparation of this manuscript; David Kemp and an un-
621 named reviewer offered important insights during the review process.

622 **References Cited**

623 Barranco, F.T. Jr., Balsam, W.L., and Deaton, B.C. (1989) Quantitative reassessment of brick
624 red lutites: Evidence from reflectance spectrophotometry. Marine Geology, 89, 299-314.
625 Balsam, W.L., and Deaton, B.C. (1991) Sediment dispersal in the Atlantic Ocean: Evaluation by
626 visible light spectra. Reviews in Aquatic Sciences, 4, 411-447.
627 Balsam, W.L., and Damuth, J.E. (2000) Further investigations of shipboard Vs shore-based
628 spectral data: Implications for interpreting Leg 164 sediment composition. In C.K. Paull,
629 R. Matsumoto, P.J. Wallace, and W.P. Dillon, Eds., Proceedings Ocean Drilling Program
630 Scientific Results. 164, p. 313 – 324. College Station, TX.
631 Balsam, W.L., and Wolhart, R. (1993) Sediment dispersal in the Argentine Basin: evidence from
632 visible light spectra. Deep-Sea Research, 40, 1001-1031.
633 Balsam, W.L., Deaton, B.C., and Damuth, J.E. (1999) Evaluating optical lightness as a proxy for
634 carbonate content in marine sediment cores: Implications for marine sedimentation.
635 Marine Geology, 161, 141-153.
636 Balsam, W.L., Ji, J., and Chen, J. (2004) Climatic interpretation of the Luochuan and Lingtai
637 loess section, China, based on changing iron oxide mineralogy. Earth and Planetary
638 Science Letters, 223, 335-348.
639 Barrón, V., and Torrent, J. (1986) Use of the Kubelka-Munk theory to study the influence of iron
640 oxides on soil colour. Journal of Soil Science, 37, 499-510.
641 Bigham, J.M., Golden, D.C., Bowen, L.H., Buol, S.W., and Weed, S.B. (1978) Iron oxide
642 mineralogy of well-drained ultisols and oxisols: I. Characterization of iron oxides in soil

clays by Mossbauer spectroscopy, X-ray diffractometry, and selected chemical techniques. Journal of American Soil Science Society, 42, 816-825.

Biscaye, P.E. (1965) Mineralogy and sedimentation of recent deep-sea clays in the Atlantic Ocean and adjacent seas and oceans. Geological Society of America Bulletin, 76, 803-832.

Brown, G., and Wood, I.G. (1985) Estimation of iron oxides in soil clays by profile refinement combined with differential X-ray diffraction. Clay Minerals, 20, 15-27.

Christensen, P.R., Morris, R.V., Lane, M. D., Bandfield, J.L., and Malin, M.C. (2001) Global mapping of Martian hematite mineral deposits: Remnants of water-driven processes on early Mars. Journal of Geophysical Research, 106, E10, 23,873–23,885.

Clark, R.N. (1999) Spectroscopy of Rocks and Minerals, and Principles of Spectroscopy (http://speclab.cr.usgs.gov) derived from Chapter 1, A. Rencz, Ed., Manual of Remote Sensing. John Wiley and Sons, Inc., New York. (http://speclab.cr.usgs.gov/PAPERS.refl-mrs/refl4.html)

Clark, R.N., and Roush, T.L. (1984) Reflectance spectroscopy: Quantitative analysis techniques for remote sensing applications, Journal of Geophysical Research, 89, 6329-6340.

Cornell, R.M., and Schwertmann, U. (2003) The iron oxides: Structure, properties, reactions, occurrences and uses, 703 p. Wiley-VCH, Weinheim.

Deaton, B.C. (1987) Quantification of rock color from Munsell chips. Journal of Sedimentary Petrology, 57, 774-776.

Deaton, B.C., and Balsam, W.L. (1991) Visible spectroscopy - a rapid method for determining hematite and goethite concentration in geological materials. Journal of Sedimentary Petrology, 61, 628-632.

Deaton, B.C., Nestell, M., and Balsam, W.L. (1996) Spectral reflectance of conodonts: A step toward quantitative color alteration and thermal maturity indexes. American Association of Petroleum Geology Bulletin, 80, 999-1007.

Dermatas, D., Chrysochoou, M., Pardali, S., and Grubb, D.G. (2007) Influence of X-ray diffraction sample preparation on quantitative mineralogy: Implications for chromate waste treatment. Journal of Environmental Quality, 36, 487-497.

Goethe, J.W. (1810) Theory of Colours, 153p. http://www.farben-welten.de/farben-welten/downloads.html (in German). English translation (2006) Dover Publications. Mineola, NY.

Griffen, G.M. (1962) Regional clay-mineral facies-product of weathering intensity and current distribution in the northeastern Gulf of Mexico. Geological Society of America Bulletin, 73, 737–768.

Hillier, S. (2003) Quantitative analysis of clay and other minerals in sandstones by X-ray powder diffraction (XRPD), In R. H. Worden and S. Morad, Eds., Clay Mineral Cements in Sandstones, p. 213–251. International Association of Sedimentologists, New York, N.Y.

Hsu, C.-P. (1997) Infrared spectroscopy. In F. Settle, Ed., Handbook of Instrumental Techniques for Analytical Chemistry, p. 247-277. Prentice-Hall, Upper Saddle River, New Jersey.

Judd, D.B., and Wyszecki, G. (1975) Color in business, science and industry, 3rd ed., 576p. John Wiley and Son, New York.

Ji, J., Balsam, W.L., and Chen, J. (2002) Rapid and precise measurement of hematite and goethite concentrations in the Chinese loess sequences by diffuse reflectance spectroscopy. Clays and Clay Minerals, 50, 210-218.

Ji, J., Chen, J., Jin, L, Zhang, W., Balsam, W.L., and Lu, H. (2004) Relating magnetic susceptibility to the simulated TM bands of the Chinese loess: the application of TM image for soil MS mapping on the Loess Plateau. Journal of Geophysical Research, 109, B05102, doi:10.1029/2003JB002769, 2004

Kampf, N., and Schwertmann, U. (1983) Goethite and hematite in a climosequence in southern Brazil and their application in classification of kaolinitic soils. Geoderma, 29, 27–39.

Kubelka, P. (1948) New contributions to the optics of intensely light-scattering materials: Part I. Journal of the Optical Society of America, 38, 448–457.

Kubelka, P., and Munk, F. (1931) A contribution to the appearance of paints. Journal of Technical Physics, 12, 593–601 (in German).

Laamanen, H., Jääskeläinen, T., and Parkkinen. J. (2005) Conversion between the reflectance spectra and the Munsell notations. COLOR research and application, 31, 57-66.

Moore, D.M., and Reynolds Jr, R.C. (1997) X-ray diffraction and the identification and analysis of clay minerals (2nd ed.), 400 p. Oxford University Press, New York.

Morris, R.V., and Lauer, H.V. Jr. (1990) Matrix effects for reflectivity spectra of dispersed nanophase (superparamagnetic) hematite with application to Martian spectral data. Journal of Geophysical Research, 95, B4, 5101–5109.

Morris, R.V., Golden, D.C., and Bell III, J.F. (1997) Low temperature reflectivity spectra of red hematite and the color of Mars. Journal of Geophysical Research, 102, E4, 9125-9133.

Munsell, A.H. (1905) A Color Notation: A measured color system based on the three qualities Hue, Value, and Chroma. 89 p., George H. Ellis and Company, Boston. (Available from Project Gutenberg at http://www.gutenberg.org/files/26054/26054-h/26054-h.htm.).

Newton, I. (1672) A Serie's of Quere's propounded by Mr. Isaac Newton … positively concluding his new Theory of Light and Colours. Philosophical Transactions of the Royal Society, No. 85 (15 July 1672), p. 5004-5007. (Available online from: http://www.newtonproject.sussex.ac.uk/view/texts/xml/NATP00014)

O'Connor, B.H., and Chang, W.J. (1986) The amorphous character and particle-size distributions of powders produced with the micronizing mill for quantitative x-ray-powder diffractometry. X-Ray Spectrometry, 5, 267-270.

Pilatti, M.A., Ghiberto, P.J., and Imhoff, S. (2006) Application of a general relationship between soil particle density and organic matter to mollisols of Santa Fe (Argentina). 18th World Congress of Soil Science, paper 163-11. Philadelphia, PA, USA.

Sabins, F. (1999) Remote sensing for mineral exploration. Ore Geology Reviews, 14, 157-183.

Scheinost, A.C., Chavernas, A., Barrón, V., and Torrent, J. (1998) Use and limitations of the second-derivative diffuse reflectance spectroscopy in the visible to near-infrared range to identify and quantify Fe oxide minerals in soils. Clays and Clay Minerals, 46, 528−536.

Schwertmann, U. (1987) Occurrence and formation of iron oxides in various pedoenvironments. In J.W. Stucki, Ed., Iron in soils and clay minerals, p. 267–308. Reidel, Norwell, MA.

Schwertmann, U., and Taylor, R.M. (1989) Iron oxides. In J.B.Dixon and S.E. Weed Eds., Minerals in Soil Environments 2nd ed. p. 379 – 438. Soil Science Society of America, Madison WI, USA.

Shields, J.A., Paul, E.A., St. Arnaud, R.J., and Head, W.K. (1968) Spectrophotometric measurement of soil color and its relationship to moisture and organic matter. Canadian Journal of Soil Science, 68, 271-280.

Simmons, E.L. (1972) Relation of the diffuse reflectance remission function to fundamental optical parameters. Optica Acta, 19, 845-851.

Torrent, J., Schwertmann, U., Fechter, H., and Alferez, F. (1983) Quantitative relationships between soil color and hematite content. Soil Science, 136, 354-358.

Torrent, J., and Barrón V. (2002) Diffuse reflectance spectroscopy of iron oxides. In A.T. Hubbard, Ed., p. 1438 – 1446. Encyclopedia of Surface and Colloid Science, Taylor and Francis, New York.

Torrent, J., Liu Q., Bloemendal J., and Barrón, V. (2007) Magnetic Enhancement and Iron oxides in the Upper Luochuan Loess-Paleosol Sequence, Chinese Loess Plateau. Soil Science Society of America Journal, 71, 1570 – 1578.

Wenlandt, W.W., and Hecht, H.G. (1966) Reflectance Spectroscopy. 298 p. Wiley-Interscience, New York.

Winters, E. (1930) The measurement of soil color. American Soil Survey Association Bulletin, 11, 34-37.

Zhang, Y., Ji, J., Balsam, W.L., Liu, L., and Chen, J. (2007) High resolution hematite and goethite records from ODP 1143, South China Sea: Co-evolution of monsoonal precipitation and El Niño over the past 600,000 years. Earth and Planetary Science Letters, 264, 136-150.

Zhou, W, Ji, J., Balsam, W.L., and Chen, J. (2010) Thermal identification of goethite and hematite by diffuse reflectance spectroscopy. Geoderma, 155, 419-425.

752 **Table 1.** Sample composition by matrix and hematite content. The bold numbers refer to the sample number used in this study. The
753 simulated North Atlantic matrix contains silica, carbonate, and illite in the ratio 4/3/3; the Gulf matrix contains carbonate, silica, and
754 illite in the ratio 5/3/2. The text contains additional details of matrix composition.
755
756

		← Percentage Mixed Hematite →							
		0	0.01	0.05	0.1	0.5	1	2	4
Base Matrix	**Other Minerals Added to Base**	← **Sample Number** →							
Carbonate		**1**	**2**	**3**	**4**	**5**	**6**	**7**	**8**
Silica		**9**	**10**	**11**	**12**	**13**	**14**	**15**	**16**
Carb/Sil		**17**	**18**	**19**	**20**	**21**	**22**	**23**	**24**
	10% Illite	**25**	**26**	**27**	**28**	**29**	**30**	**31**	**32**
	25% Illite	**33**	**34**	**35**	**36**	**37**	**38**	**39**	**40**
	50% Illite	**41**	**42**	**43**	**44**	**45**	**46**	**47**	**48**
North Atlantic	1% Chlorite	**49**	**50**	**51**	**52**	**53**	**54**	**55**	**56**
	5% Chlorite	**57**	**58**	**59**	**60**	**61**	**62**	**63**	**64**
	15% Chlorite	**65**	**66**	**67**	**68**	**69**	**70**	**71**	**72**
Gulf	1% Kaolinite	**73**	**74**	**75**	**76**	**77**	**78**	**79**	**80**
	5% Kaolinite	**81**	**82**	**83**	**84**	**85**	**86**	**87**	**88**
	15% Kaolinite	**89**	**90**	**91**	**92**	**93**	**94**	**95**	**96**
	1% Montmorillonite	**97**	**98**	**99**	**100**	**101**	**102**	**103**	**104**
	5% Montmorillonite	**105**	**106**	**107**	**108**	**109**	**110**	**111**	**112**
	15% Montmorillonite	**113**	**114**	**115**	**116**	**117**	**118**	**119**	**120**

757
758
759
760

Table 2. Sources of material used to make the samples.

Source Materials		
Hematite	Pfizer R-1599 Pure red iron oxide	Lot E3044
$CaCO_3$	Baker reagent 1288-05	Lot D29353
Silica (SiO_2)	Aldrich	Lot 02315MX
Illite	API#35	Fifthian, IL
Chlorite (ripidolite)	Clay Mineral Repository	Flagstaff Hill, El Dorado City, CA
Kaolinite	API#9	Mesa Alta, NM
Montmorillonite (Na-Ca; beidellite)	API#31	Cameron, AZ

Table 3. Results of visual test of hematite discrimination in different matrices. The matrices are arranged from lightest to darkest starting with 0% hematite. The Gulf matrix contains 15% montmorillonite and the North Atlantic matrix contains 15% chlorite. There were 24 participants in the test.

Matrix/ %Hematite	%Seeing Red
Carb 0%	0.0
Carb 0.01%	95.8
Carb 0.05%	100.0
Carb 0.1%	95.8
Carb 0.5%	100.0
Carb/Sil 0%	8.3
Carb/Sil 0.01%	62.5
Carb/Sil 0.05%	100.0
Carb/Sil 0.1%	100.0
Carb/Sil 0.5%	100.0
Gulf 0%	8.3
Gulf 0.01%	12.5
Gulf 0.05%	29.2
Gulf 0.1%	62.5
Gulf 0.5%	100.0
North Atlantic 0%	4.2
North Atlantic 0.01%	8.3
North Atlantic 0.05%	8.3
North Atlantic 0.1%	20.8
North Atlantic 0.5%	100.0

Figure Captions

Figure 1. (**a)** Slides of mixed samples in 4 different matrices of calcium carbonate/silica, 1:1, mixed with differing concentrations of illite and 8 different concentrations of hematite including 0%. Note that as the matrix gets darker with the addition of illite the detection limit of hematite increases. Samples 17 – 48 (Table 1) are illustrated on this figure. (**b)** Slides of mixed samples in the North Atlantic matrix (silica, carbonate, and illite in the ratio 4/3/3) with varying concentrations of hematite and chlorite. Samples 49 – 72 (Table 1) are illustrated on this figure. Similar to the experiments with increasing illite concentration, increasing chlorite concentration makes hematite more difficult to detect. The color of the samples shown on the following figures only approximates direct visual observation. The subtlety of the color variation shown by the samples is nearly impossible with to reproduce even adjusting for color temperature of the lighting and bracketing exposures. In addition, the fidelity of the images is further degraded preparing them for publication or by printing them.

Figure 2. X-ray spectrum of 1% hematite in the Gulf matrix with 1% kaolinite (sample 78, Table 1). Peaks attributable to quartz, calcite and ZnO are labeled. The primary hematite peaks are indicated by arrows. These peaks are so small that hematite would likely not be identified by most analysts. The 1% kaolinite in this sample is below the detection limit of XRD in this matrix.

Figure 3. Example of changes in spectral percent reflectance curves with both changing matrices and hematite content. Zero percent hematite is the matrix with no hematite added to it. (**a**) is a light matrix of calcite and silica (samples 17 – 24, Table 1) whereas (**b**) is a dark matrix (samples 65 – 72, Table 1).

Figure 4. (**a**) Percent hematite as a function of percent reflectance in the red color band, 630 – 700 nm, for the seven data sets shown in Figure 1. (**b)** Percent hematite as a function of percent reflectance in the red color band for all 120 samples in the calibration data set. (**c)** Percent hematite as a function of percent reflectance in the orange color band, 590 - 630 nm, for all 120 samples in the calibration data set. Note that both the r^2 and SEE for orange are better than for the red color band.

Figure 5. First derivative of the percent reflectance data (Figure 3) from the two matrix series presented (Figures 1a and b). Note that for each matrix the height of the first derivative peak increases with increasing hematite concentration up to 1% in a light matrix (**a**) and 4% in a darker matrix (**b**).

Figure 6. Kubelka-Munk remission function applied to percent reflectance spectra from the two matrix series [carbonate/ silica matrix (**a**) and North Atlantic matrix (**b**)] illustrated on Figures 1 and 3. Note how the K-M function compresses the red end of the spectrum and expands the blue end.

Figure 7. First derivative of the K-M function for the carbonate/ silica matrix (**a**) and North Atlantic matrix (**b**). The lowest concentration of hematite that can be easily detected by the first derivative of the K-M function is 0.5% in contrast to first derivative curves (Figure 5) with a limit of 0.05% or less.

Figure 8. Second derivative of the K-M function for the carbonate/silica matrix (**a**) and North Atlantic matrix (**b**).

Figure 9. Examples of the "matrix effect". All the illustrated samples (samples 4, 12, 28,60, 84,and 108 on Table 1) contain 0.1% hematite, but are in different matrices. Note the variation in color and the changing ability to detect hematite in differing matrices.

838 **Figure 10.** Relationship between %hematite and the ratio of the percent reflectance in the green
839 versus red color bands for all 120 samples. Taking the ratio of color bands slightly improves the
840 ability to estimate hematite concentration compared to only the red color band. V1 in the
841 equation refers to the ratio of green to red color bands.

842
843
844
845 # Figures
846
847 Figure 1 (a)
848
849

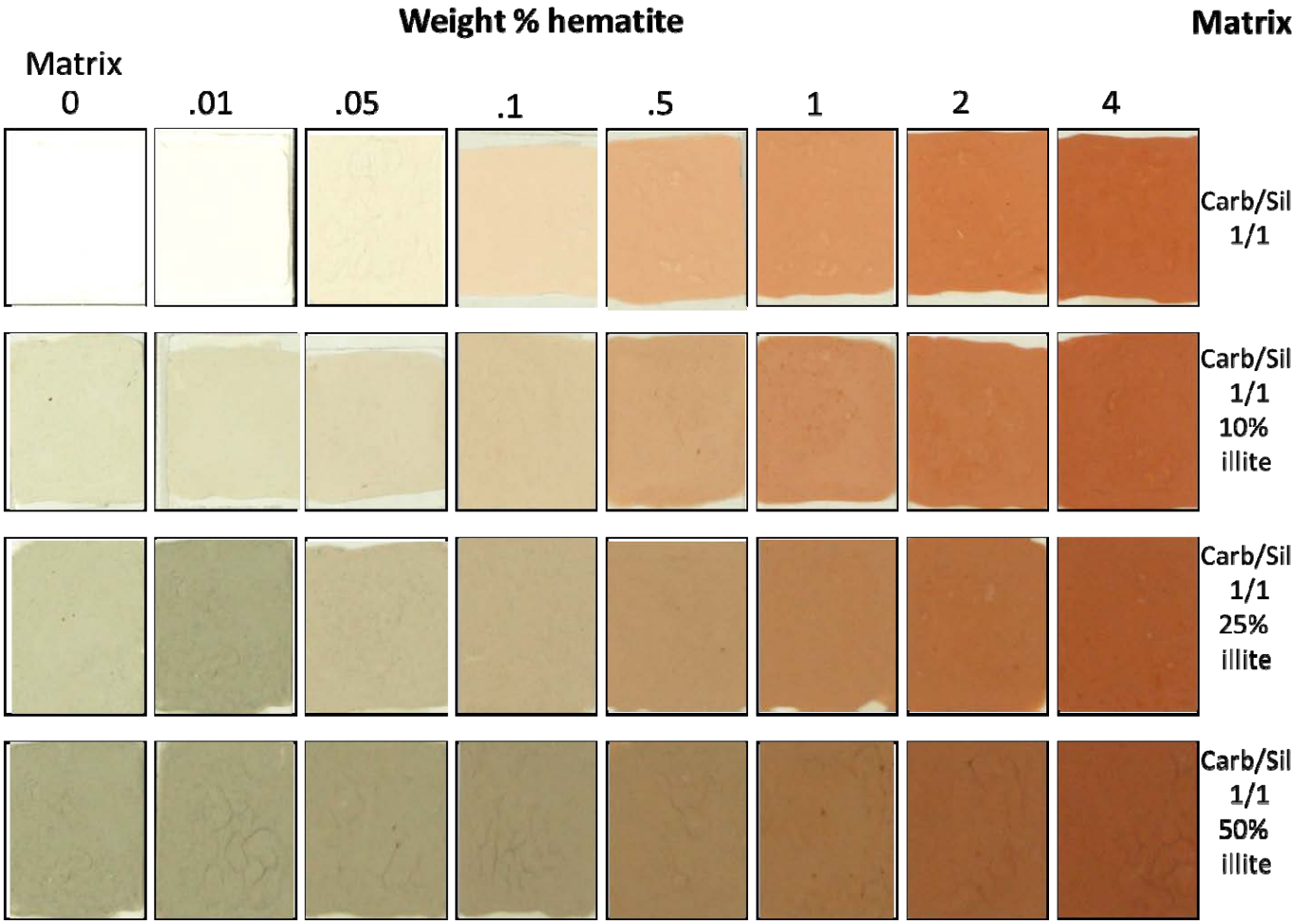

850
851
852
853

Figure 1 (b)

Figure 2

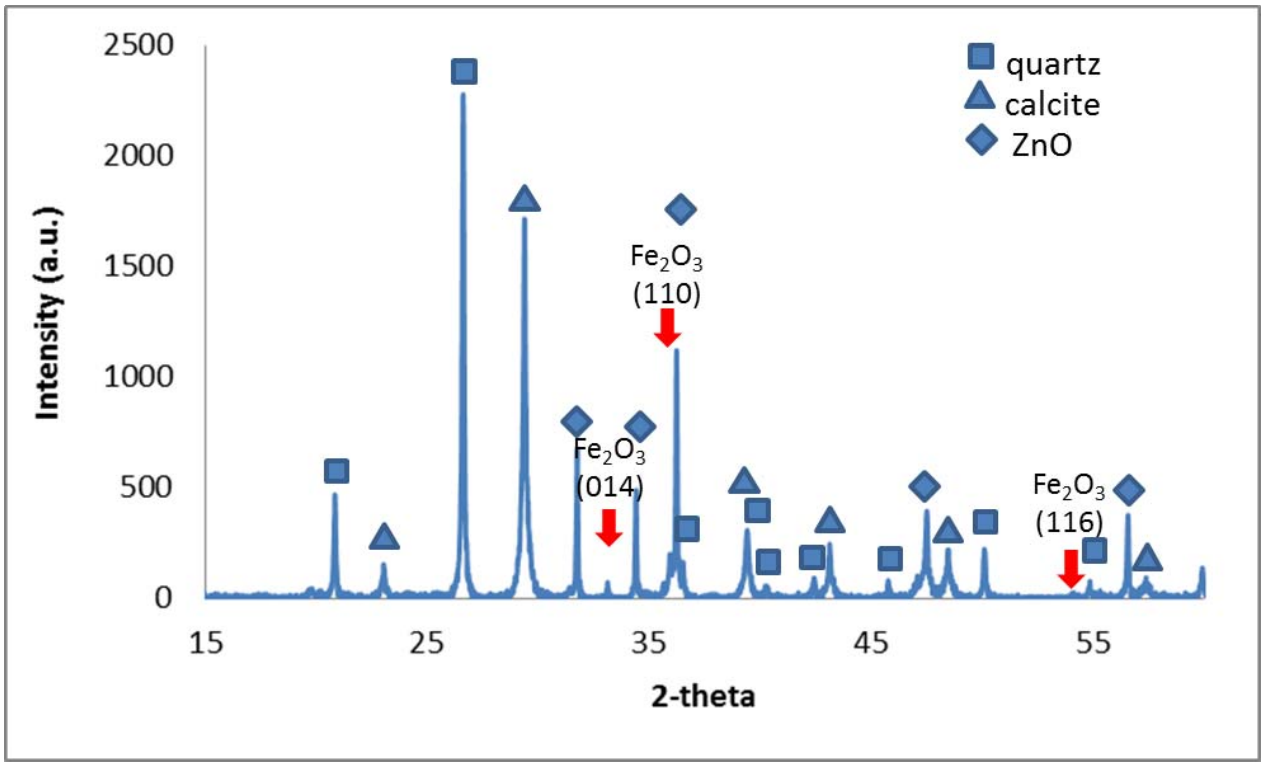

Figure 3.

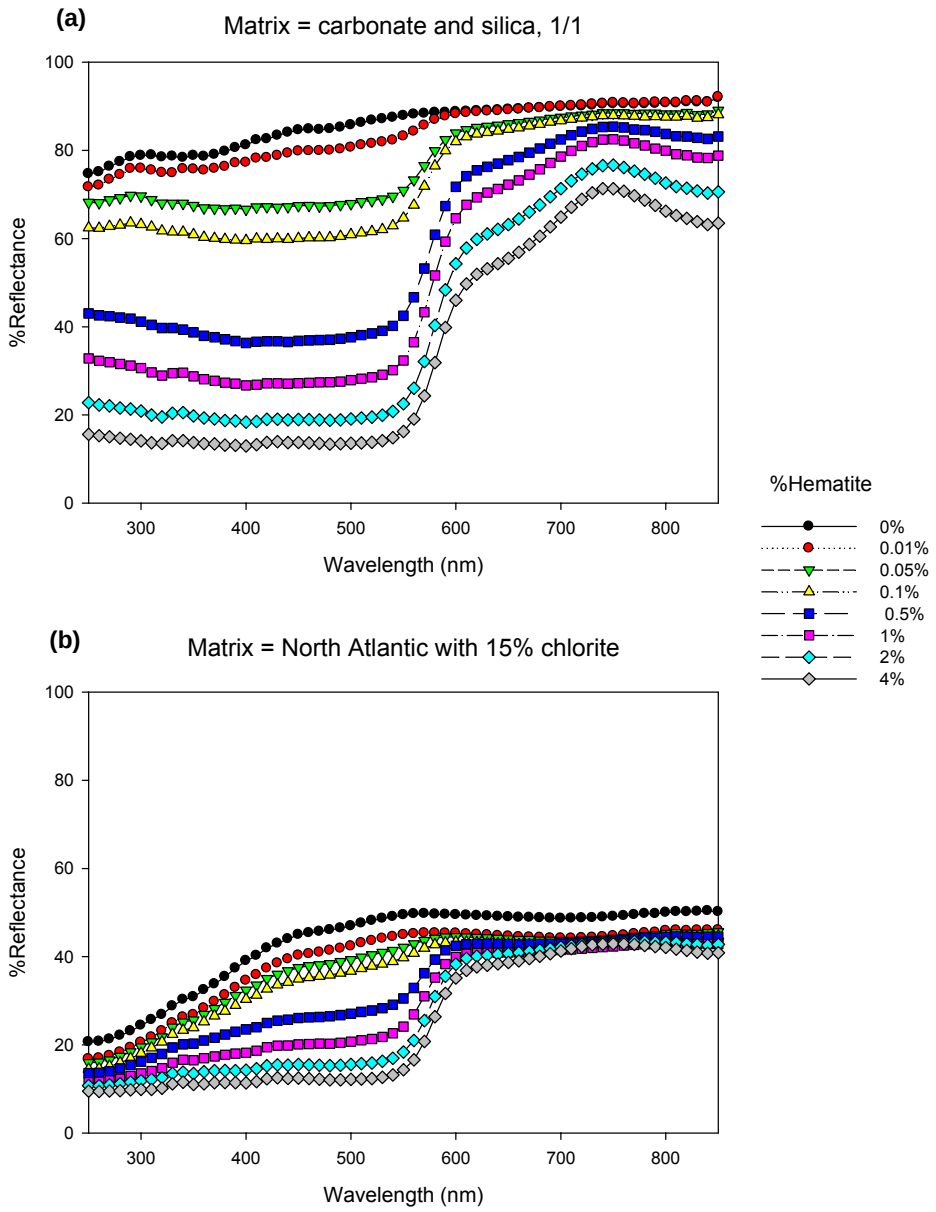

879

880 Figure 4(a)

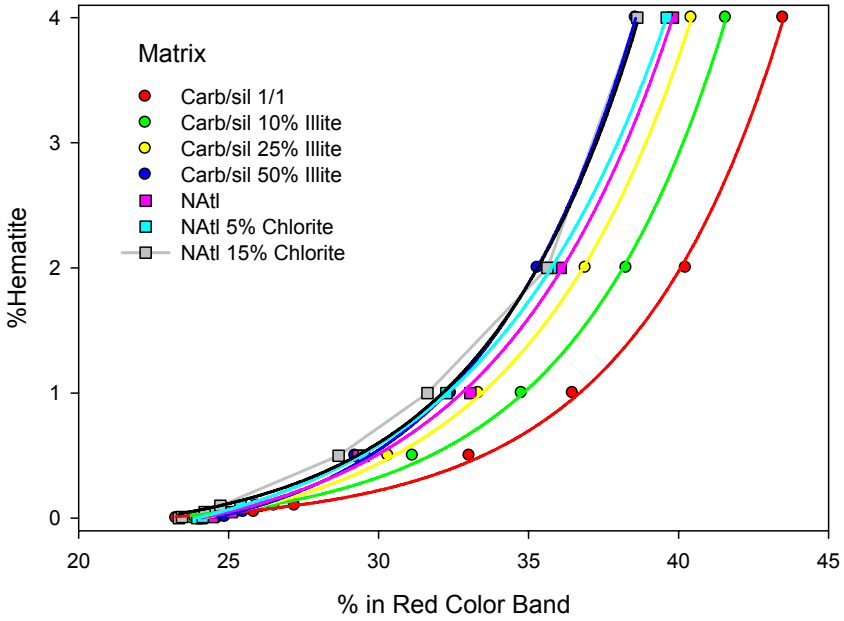

881 Figure 4(b)

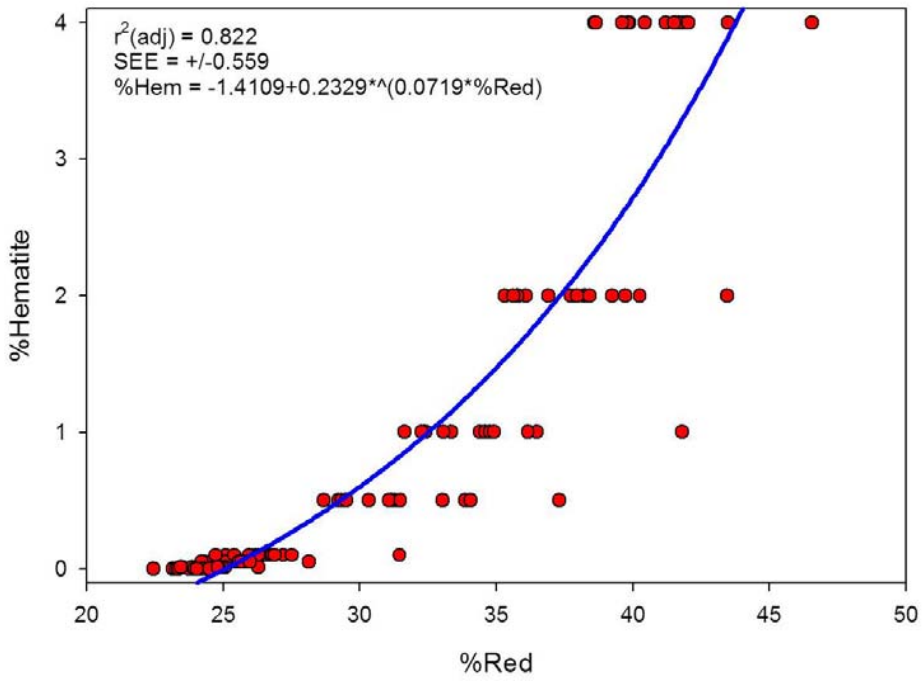

882
883
884

885

886 Figure 4(c)

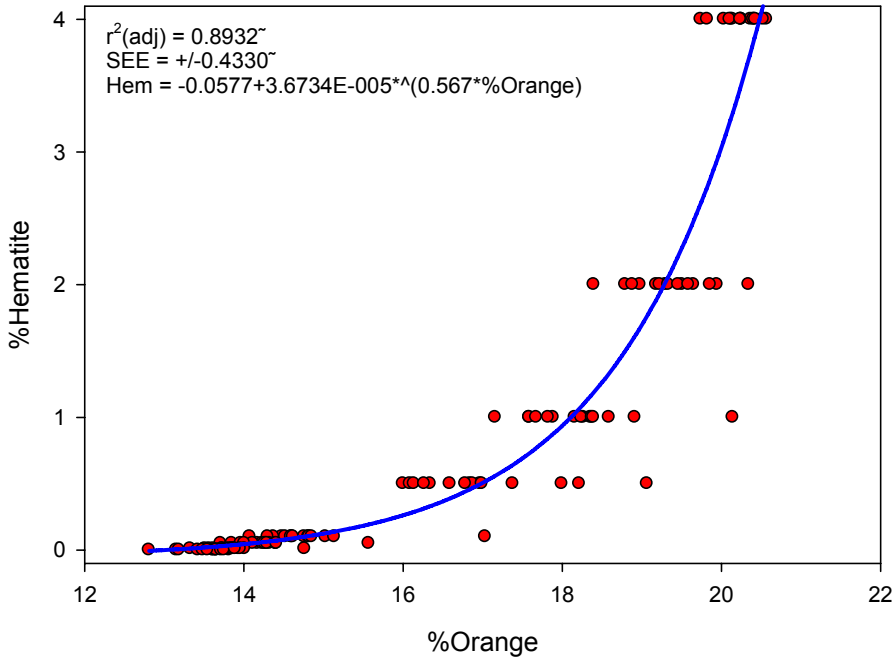

887
888
889
890

Figure 5.

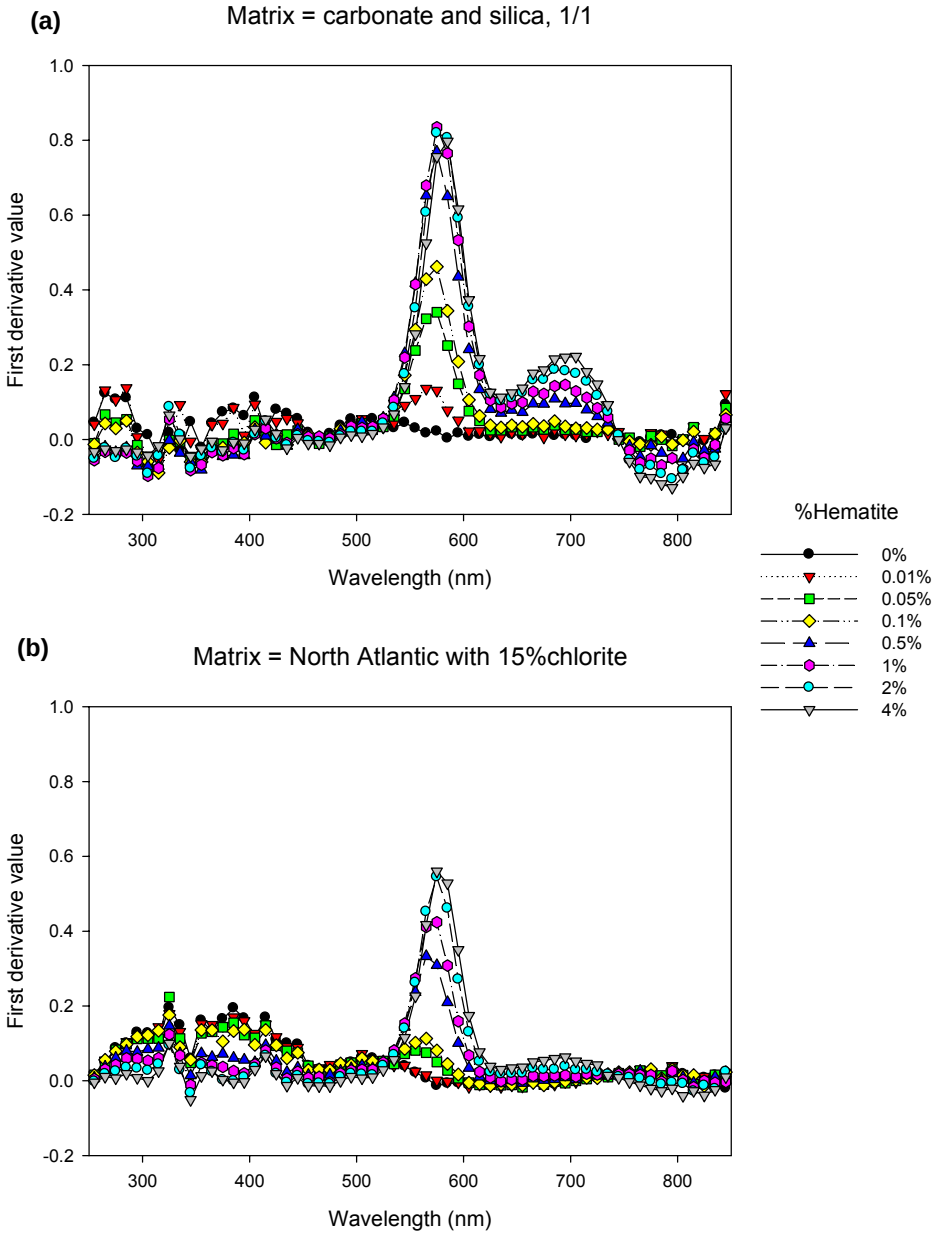

Figure 6.

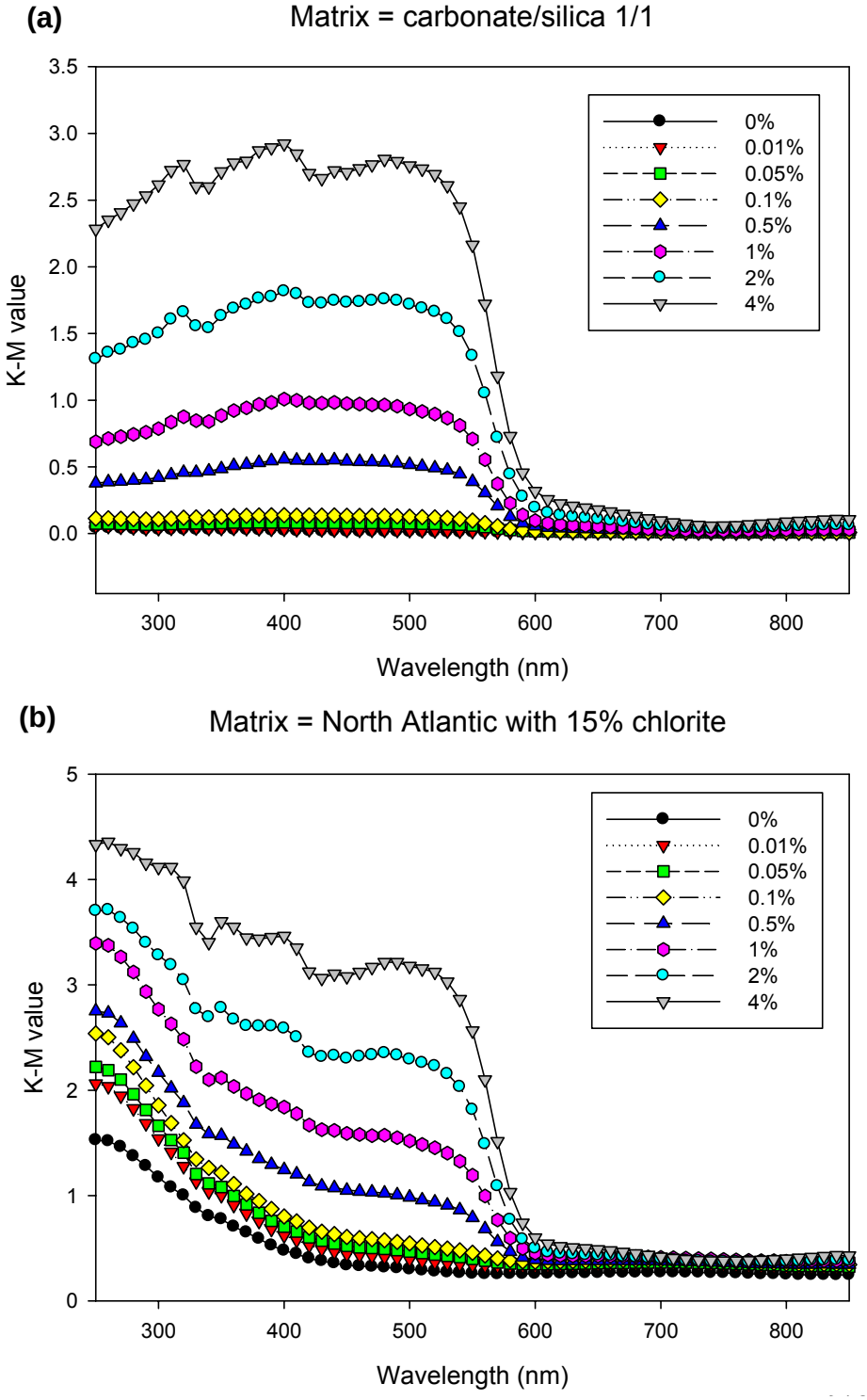

Figure 7.

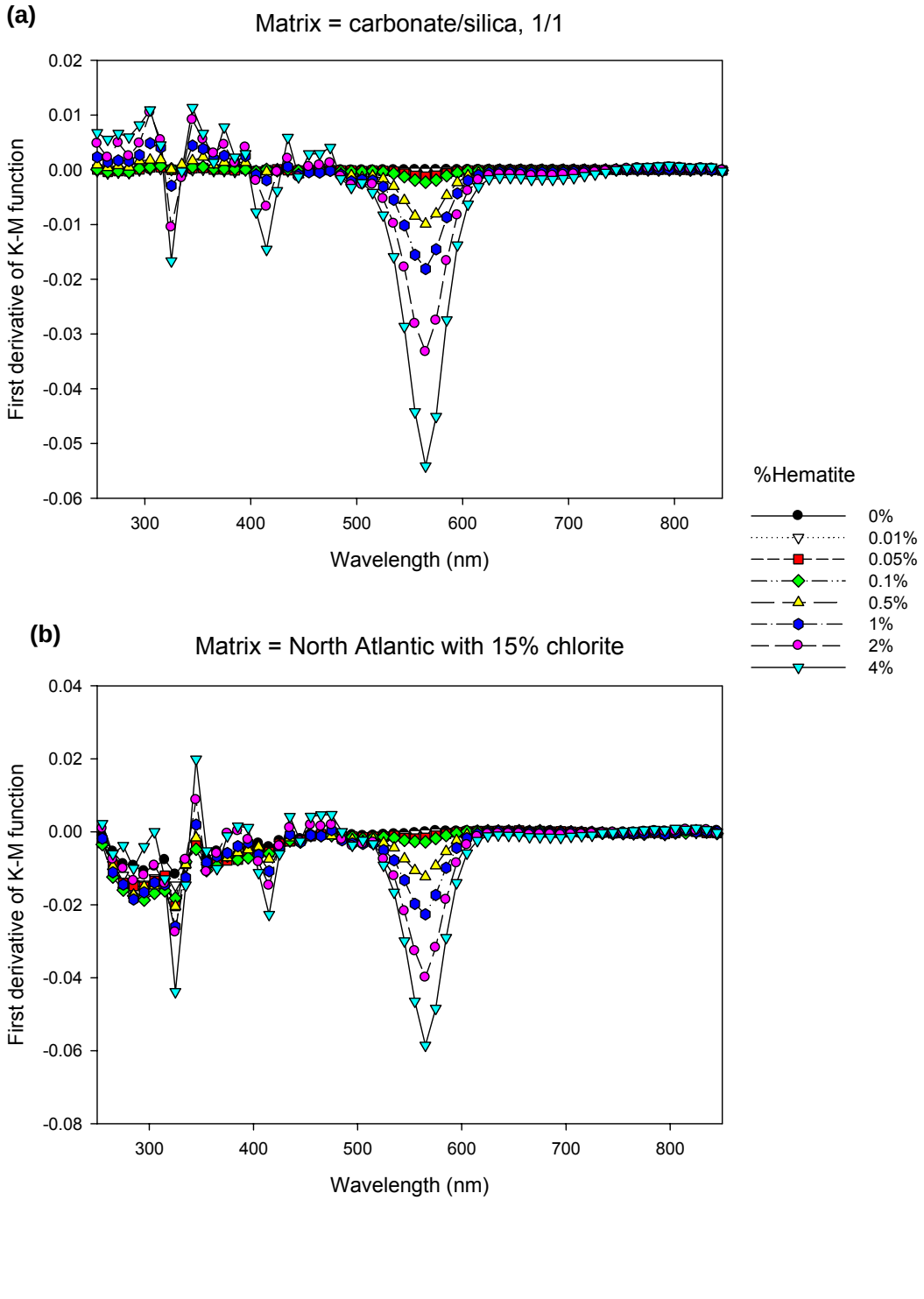

Figure 8.

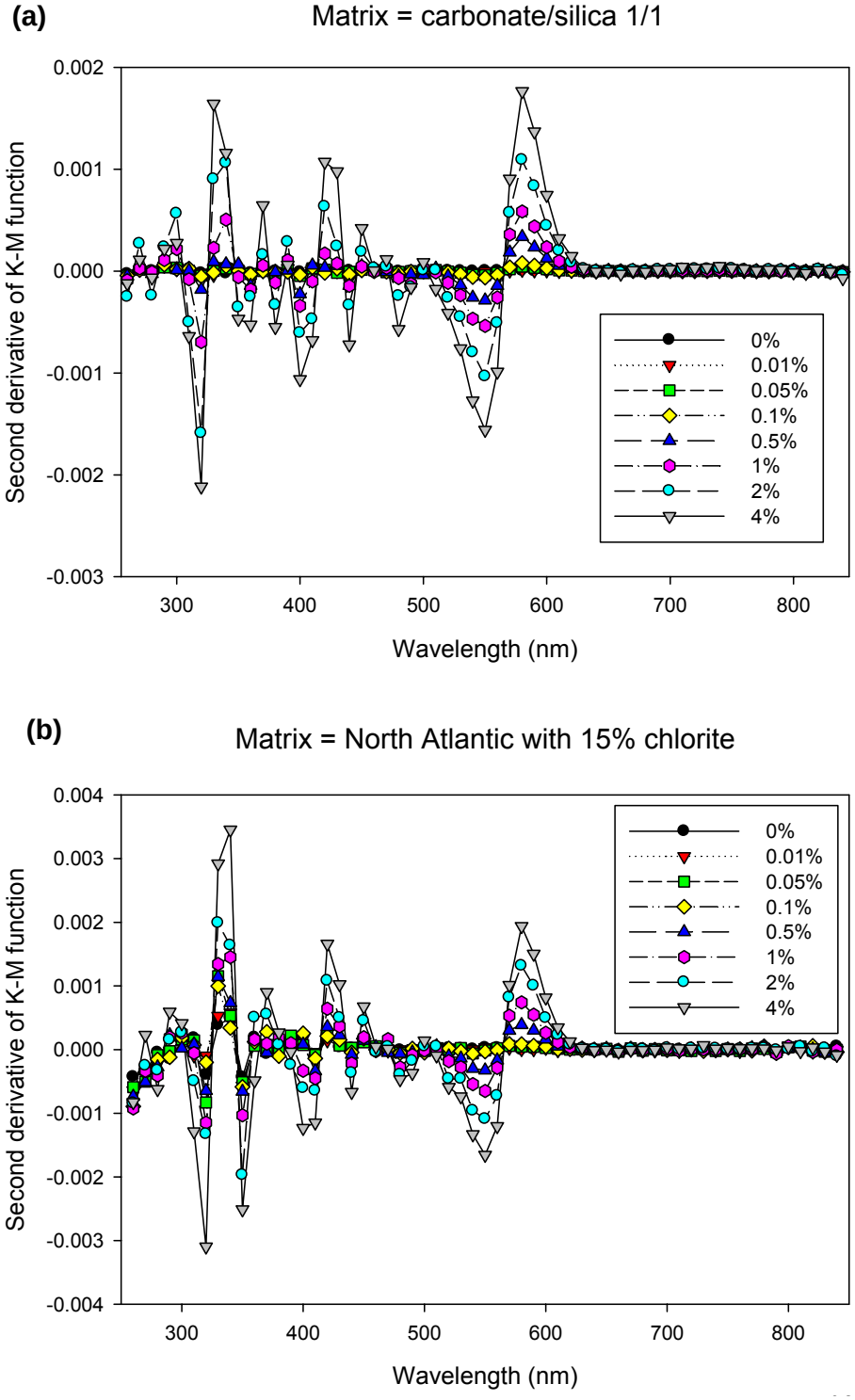

1072
1073 Figure 9.

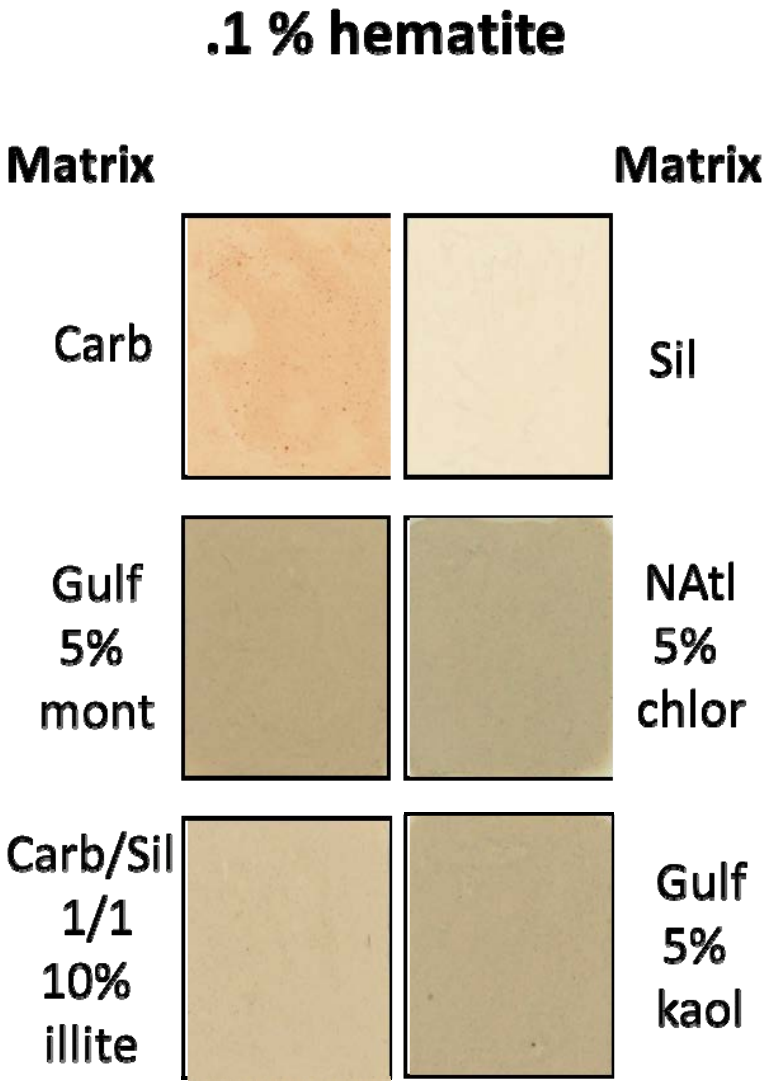

1074
1075
1076
1077
1078

Figure 10.